Journal of Medicinal Chemistry

Article

pubs.acs.org/jmc

1,2,3-Triazole-Containing Uracil Derivatives with Excellent Pharmacokinetics as a Novel Class of Potent Human Deoxyuridine Triphosphatase Inhibitors

Hitoshi Miyakoshi,[†,§] Seiji Miyahara,[†,‡] Tatsushi Yokogawa,[†] Kanji Endoh,[†] Toshiharu Muto,[†] Wakako Yano,[†] Takeshi Wakasa,[†] Hiroyuki Ueno,[†] Khoon Tee Chong,[†] Junko Taguchi,[†] Makoto Nomura,[†] Yayoi Takao,[†] Akio Fujioka,[†] Akihiro Hashimoto,[†] Kenjirou Itou,[†] Keisuke Yamamura,[†] Satoshi Shuto,[‡] Hideko Nagasawa,[§] and Masayoshi Fukuoka*[,†]

[†]Drug Discovery Research Center, Taiho Pharmaceutical Co. Ltd., Okubo 3, Tsukuba, Ibaraki 300-2611, Japan

[‡]Faculty of Pharmaceutical Sciences, Hokkaido University, Kita-12, Nishi-6, Kita-ku, Sapporo 060-0812, Japan

[§]Laboratory of Pharmaceutical and Medicinal Chemistry, Gifu Pharmaceutical University, 1-25-4 Daigaku-nishi, Gifu 501-1196, Japan

S *Supporting Information*

ABSTRACT: Deoxyuridine triphosphatase (dUTPase) has emerged as a potential target for drug development as a 5-fluorouracil-based combination chemotherapy. We describe the design and synthesis of a novel class of human dUTPase inhibitors, 1,2,3-triazole-containing uracil derivatives. Compound **45a**, which possesses 1,5-disubstituted 1,2,3-triazole moiety that mimics the amide bond of *tert*-amide-containing inhibitor **6b** locked in a cis conformation showed potent inhibitory activity, and its structure−activity relationship studies led us to the discovery of highly potent inhibitors **48c** and **50c** (IC_{50} = ∼0.029 μM). These derivatives dramatically enhanced the growth inhibition activity of 5-fluoro-2′-deoxyuridine against HeLa S3 cells in vitro (EC_{50} = ∼0.05 μM). In addition, compound **50c** exhibited a markedly improved pharmacokinetic profile as a result of the introduction of a benzylic hydroxy group and significantly enhanced the antitumor activity of 5-fluorouracil against human breast cancer MX-1 xenograft model in mice. These data indicate that **50c** is a promising candidate for combination cancer chemotherapies with TS inhibitors.

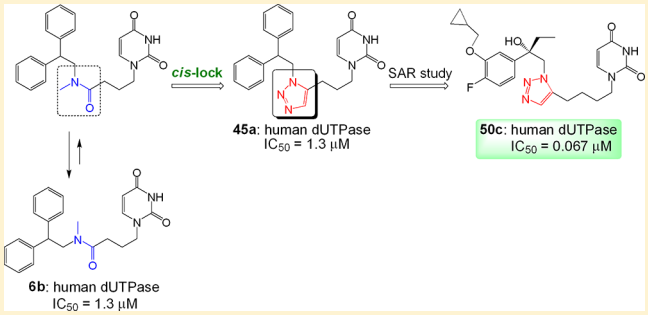

INTRODUCTION

Deoxyuridine triphosphatase (dUTPase) specifically recognizes deoxyuridine triphosphate (dUTP) among the natural nucleoside triphosphates and hydrolyzes it to deoxyuridine monophosphate (dUMP) and pyrophosphate.[1] This enzyme is thought to be responsible for two biological roles, (1) decreasing the intracellular dUTP pools to prevent misincorporation of uracil instead of thymine into DNA and (2) supplying dUMP as a substrate for thymidylate synthase (TS) for conversion to thymidine monophosphate (dTMP), an essential precursor for the de novo pathway of DNA synthesis.[2]

TS inhibitors decrease the intracellular thymidine triphosphate (dTTP) pools, resulting in thymineless death concurrently with increasing the dUMP pools, which results in expansion of intracellular dUTP pools. When 5-fluorouracil (5-FU) or its derivatives are used as a TS inhibitor, intracellular 5-fluoro-2′-deoxyuridine triphosphate (FdUTP) pool is also increased. The expansion of dUTP and FdUTP pools causes uracil and 5-FU misincorporation into DNA, which is one of the key mechanisms of the cytotoxity induced by TS inhibitors.[3−5] Accordingly, the expression of dUTPase which decomposes dUTP and FdUTP can mediate resistance to 5-FU by preventing the misincorporation of dUTP and FdUTP into DNA in cancer cells.[6−8] Therefore, we have been developing dUTPase inhibitors to enhance the antitumor effect of 5-FU based chemotherapy because dUTPase has been considered to be an attractive and potential target in a new strategy for 5-fluorouracil-based combination chemotherapy.

Although there have been extensive efforts made to develop dUTPase inhibitors (Figure 1),[9−18] to the best of our knowledge, none of them has been evaluated in clinical trials. We have already reported the development of amide-type human dUTPase inhibitors, **5**−**7**, which have potent inhibitory activity and drug-like properties compared to known compounds **1**−**4**.[19−21] Among these, compound **5** has shown the most potent inhibitory activity (IC_{50} = 0.021 μM) and the greatest ability to enhance antitumor activity of 5-FU in vivo.[20] During the development of the dUTPase inhibitors, our initial screening led to the identification of the simple amide **6b** as a hit compound

Received: March 25, 2012
Published: June 20, 2012

dx.doi.org/10.1021/jm3004174 | *J. Med. Chem.* 2012, 55, 6427−6437

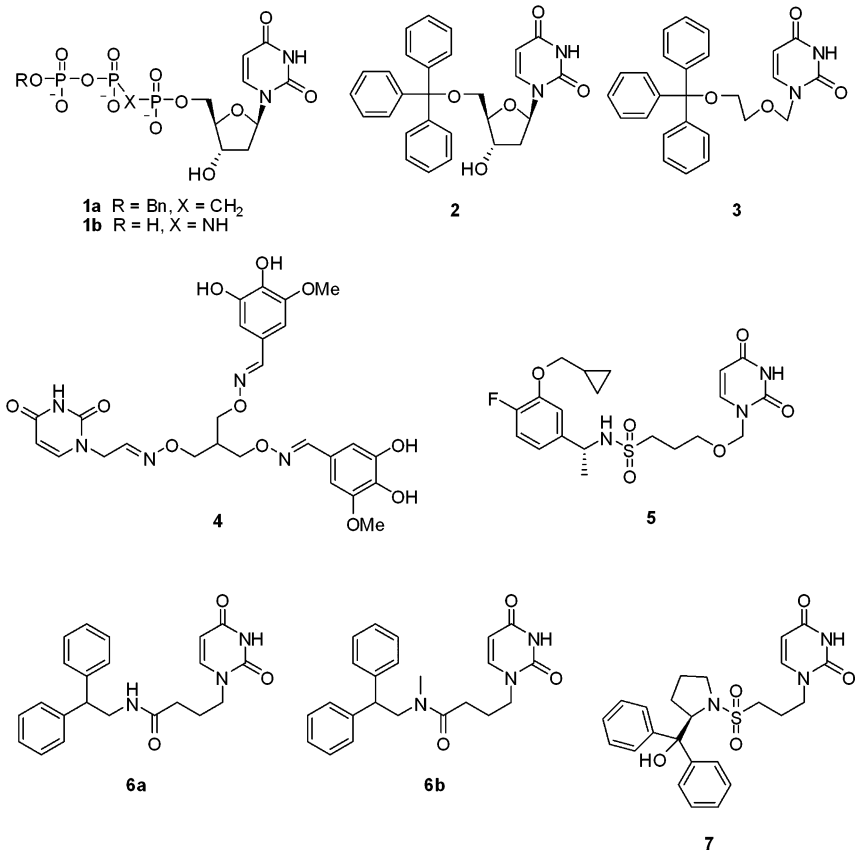

Figure 1. Structural formulas of dUTPase inhibitors.

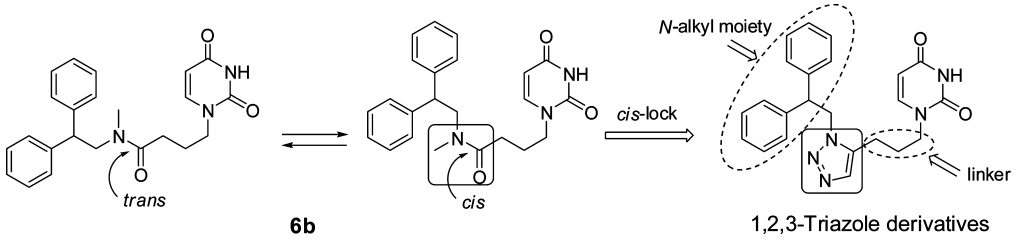

Figure 2. Triazole-replacement strategy for compound **6b** and molecular modification for the SAR study.

with a favorable level of lipophilicity and molecular weight (MW, 391; clogP, 2.17). Subsequent structure−activity relationship (SAR) studies of amide-containing uracil derivatives revealed that the *tert*-amide compound **6b** had almost 12-fold more potent inhibitory activity compared to the *sec*-amide compound **6a**.[19] We predicted from a conformational analysis by NMR that the cis conformational preference of the *tert*-amide moiety of **6b** may contribute to its greater potency.[19] On the basis of this hypothesis, we designed 1,2,3-triazole derivatives by replacing the amide moiety of **6b** with a conformationally restricted surrogate of the cis amide to further improve the inhibitory potency. These derivatives could be readily synthesized from alkyne intermediates and azide intermediates (Figure 2). From the SAR studies focused on 1,2,3-triazole-containing uracil derivatives, we have identified highly potent inhibitors of human dUTPase with IC_{50} values in the 10^{-8} M range. We also report that compound **50c** has a desirable pharmacokinetic profile in mice and clearly enhances the antitumor activity of a TS inhibitor in vivo.

In this paper, we report the details of the design and synthesis of novel 1,2,3-triazole-containing uracil compounds, their evaluation as human dUTPase inhibitors, and their ability to enhance the growth inhibition activity of a TS inhibitor against cancer cells in vitro and in vivo.

CHEMISTRY

Alkyne intermediates **9a−b** and **11** were synthesized as shown in Scheme 1. Compounds **9a−b** were prepared by the Mitsunobu reaction of commercially available 4-pentyn-1-ol **8b** or 4-pentyn-1-ol **8c** and 3-*N*-benzoyluracil,[22] followed by the removal of the benzoyl group with methylamine. Compound **11** was synthesized in two steps. Commercially available 3-butyn-1-ol **8a** was treated with chloromethylmethylether to provide **10**. The methoxymethyl (MOM) group of **10** was activated with BCl_3 and was then treated with $(TMS)_2$Ura and a catalytic amount of iodine to give **11**.[23]

The synthesis of azide intermediates **14a−d** is shown in Scheme 2. The phenolic group of **12a−b** was alkylated with (bromomethyl)cyclopropane to provide **13c−d**. Commercially available **13a−b** and intermediates **13c−d** were treated with MsCl and then with NaN_3 to give **14a−d**.

dx.doi.org/10.1021/jm3004174 | J. Med. Chem. 2012, 55, 6427−6437

Scheme 1. General Synthetic Method for Preparation of Alkyne Intermediates 9a−b and 11[a]

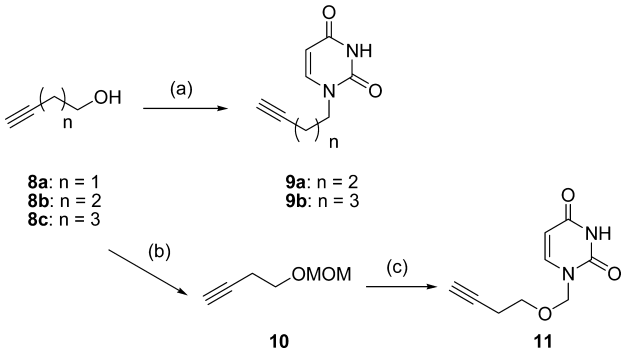

[a]Reagents and conditions: (a) *N*-3-Bz-uracil, PPh_3, DIAD, THF, room temp, 2 h then $MeNH_2$, MeOH, room temp, 1 h; (b) MOMCl, DIEA, CH_2Cl_2, room temp, 5 h; (c) BCl_3, CH_2Cl_2, room temp, 1.5 h then $(TMS)_2Ura$, I_2, DCE, 90 °C, 2 h.

Scheme 2. General Synthetic Method for Preparation of Azide Intermediates 14a−d[a]

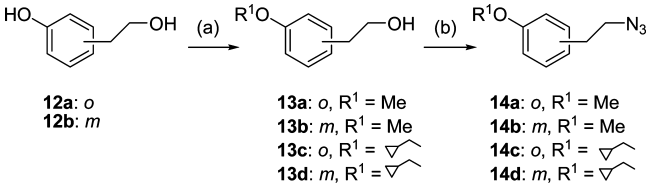

[a]Reagents and conditions: (a) (bromomethyl)cyclopropane, K_2CO_3, DMF, 90 °C, 5 h; (b) MsCl, TEA, CH_2Cl_2, room temp, 30 min then NaN_3, DMF, 50 °C, 12 h.

Azide intermediates **22a−d** were synthesized as shown in Scheme 3. Commercially available **15** was converted to ethyl ester **16**. The phenolic group of **16** was then benzylated, and the ethyl ester was hydrolyzed to give **17**. Carboxylic acid **17** was activated by $SOCl_2$, and reaction of the acyl chloride with (*R*) or (*S*)-4-benzyl-2-oxazolidine activated by *n*-BuLi provided **18a−b**. Evans asymmetric alkylation was performed on **18a−b** to afford chiral derivatives **19a−d**, respectively.[24] Removal of their benzyl groups generated the unmasked phenol groups which were then alkylated to provide **20a−f**. Reduction of **20a−f** with $LiBH_4$ produced **21a−f**. The specific rotation of **21f** was almost identical with reference data [**21f**, $[\alpha]^{25}_D = -16.1$ (*c* 1.09, $CHCl_3$); reference data,[25] $[\alpha]^{25}_D = -16.6$ (*c* 1.09, $CHCl_3$)]. Compounds **21a−d** were then converted to the corresponding azides **22a−d**.

Synthesis of azide intermediates **34a−i** is shown in Scheme 4. Commercially available **23** was treated with chloromethylmethylether to give **24**. After the hydrolysis of **24** to give **25**, a condensation reaction with MeNHOMe·HCl afforded the Weinreb amide **26**. Intermediate **26** was converted to the propiophenone derivative **27** by a Grignard reaction, and a subsequent Wittig reaction with $MePPh_3Br$ provided **28**. Compound **28** was converted to chiral derivatives **29a−b** by asymmetric dihydroxylation using AD-mixα or AD-mixβ. The primary hydroxyl group of **29a−b** was then acylated by the appropriate acyl chloride, and subsequent removal of the MOM protecting group gave crystalline compounds **31a−c**. The optical purities of **31a** and **31b** were improved to 96% ee by repeated crystallizations (three times). A single crystal X-ray structure of **31c** showed that this analogue possesses the desired *S* configuration (Figure 3). The phenolic group of **31a−b** was then alkylated via a Mitsunobu reaction or by treatment with

Scheme 3. General Synthetic Method for Preparation of Azide Intermediates 22a−d[a]

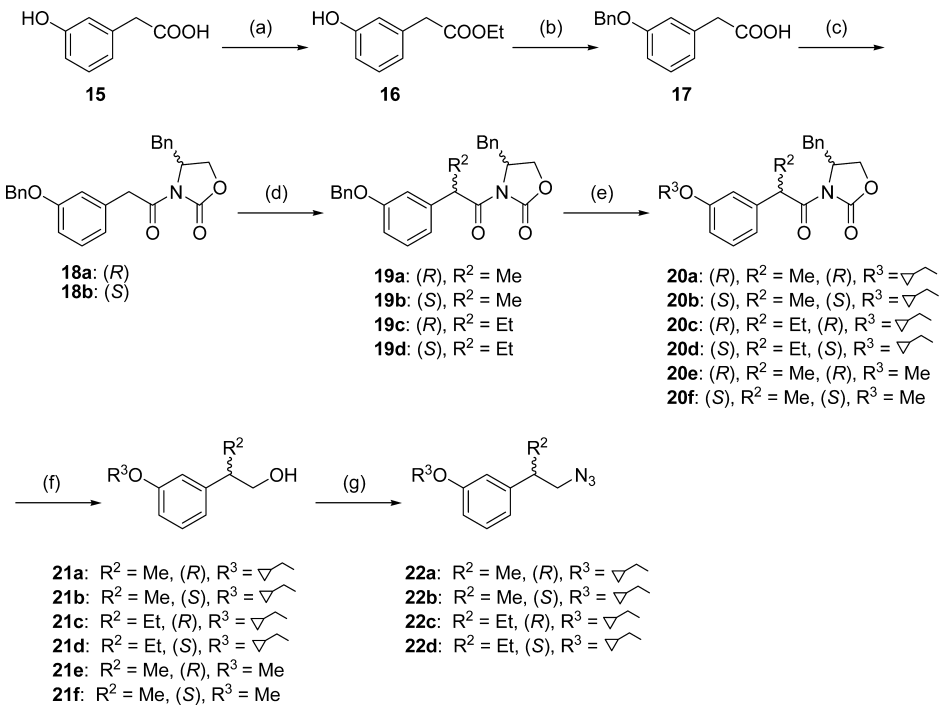

[a]Reagents and conditions: (a) H_2SO_4, EtOH, reflux, 4 h; (b) BnBr, K_2CO_3, DMF, 90 °C, 5 h then aq NaOH, EtOH, 60 °C, 4 h; (c) $SOCl_2$, DMF, 50 °C, 2 h then (*R*)- or (*S*)-4-benzyl-2-oxazolidine, *n*-BuLi, THF, 0 °C, 2 h; (d) EtI or MeI, NaHMDS, THF, −78 to −20 °C, 4−6 h; (e) $Pd(OH)_2$/C, H_2, MeOH, room temp, 1 h then (bromomethyl)cyclopropane or MeI, K_2CO_3, DMF, 70−90 °C, 2 h; (f) $LiBH_4$, THF, 0 °C, 6 h; (g) MsCl, TEA, CH_2Cl_2, room temp, 30 min then NaN_3, DMF, 60 °C, 12 h.

dx.doi.org/10.1021/jm3004174 | *J. Med. Chem.* 2012, 55, 6427−6437

Scheme 4. General Synthetic Method for Preparation of Azide Intermediates 34a−i[a]

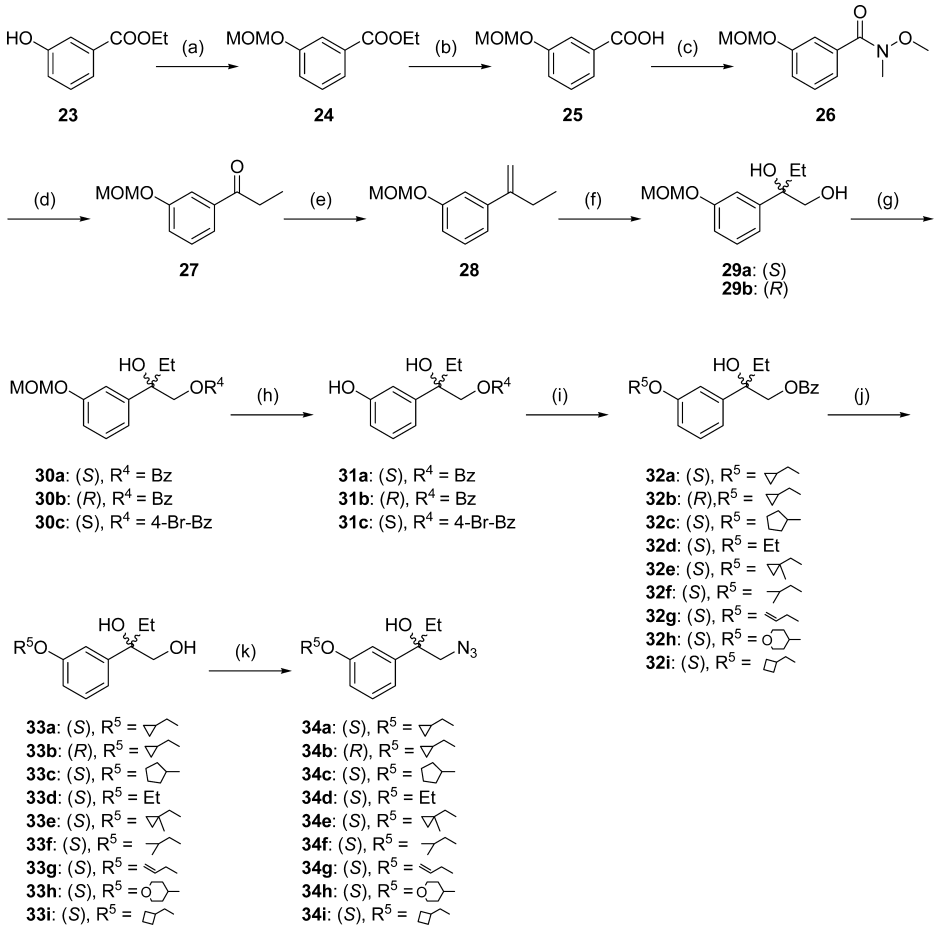

[a]Reagents and conditions: (a) MOMCl, DIEA, CH_2Cl_2, room temp, 5 h; (b) aq NaOH, EtOH, 60 °C, 4 h; (c) MeNHOMe·HCl, EDC·HCl, HOBt, TEA, DMF, room temp, 6 h; (d) EtMgBr, THF, room temp, 3 h; (e) $MePPh_3Br$, NaHMDS, THF, room temp, 12 h; (f) AD-mixα or AD-mixβ, *t*-BuOH, H_2O, 0 °C, 3 h; (g) BzCl or 4-Br-BzCl, TEA, CH_2Cl_2, room temp, 2 h; (h) aq AcOH, TFA, 50 °C, 3 h; (i) alkylbromide, K_2CO_3, DMF, 90 °C, 2−5 h or alcohol, PPh_3, DIAD, THF, room temp, 3 h; (j) aq NaOH, MeOH, 50 °C, 2 h; (k) MsCl, TEA, CH_2Cl_2, room temp, 30 min then NaN_3, DMF, 90 °C, 12 h.

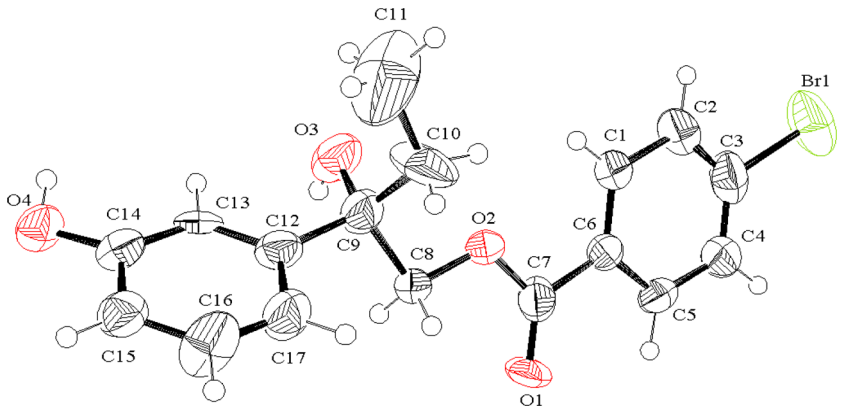

Figure 3. ORTEP view of single-crystal X-ray structure of **31c**.

alkyl halide to give the corresponding derivatives **32a−i**. The benzoyl group of **32a−i** was removed by alkaline hydrolysis to give **33a−i**, and these compounds were subsequently converted to the corresponding azides **34a−i**.

Azide intermediates **43** and **44** were synthesized as shown in Scheme 5. Commercially available **35** was treated with sulfuric acid in EtOH to give the ethyl ester, and this was followed by alkylation to give **36**. After the hydrolysis of the ethyl ester of **36**, a condensation reaction of the resulting acid with MeNHOMe·HCl afforded the Weinreb amide **38**. Compound **38** was converted to the propiophenone derivative **39** via a Grignard reaction, and **39** was then subjected to a Wittig reaction to provide **40**. Compound **40** was converted to chiral derivatives **41a−b** by asymmetric dihydroxylation using AD-mixα or AD-

dx.doi.org/10.1021/jm3004174 | *J. Med. Chem.* 2012, 55, 6427−6437

Scheme 5. General Synthetic Method for Preparation of Azide Intermediates 43, 44[a]

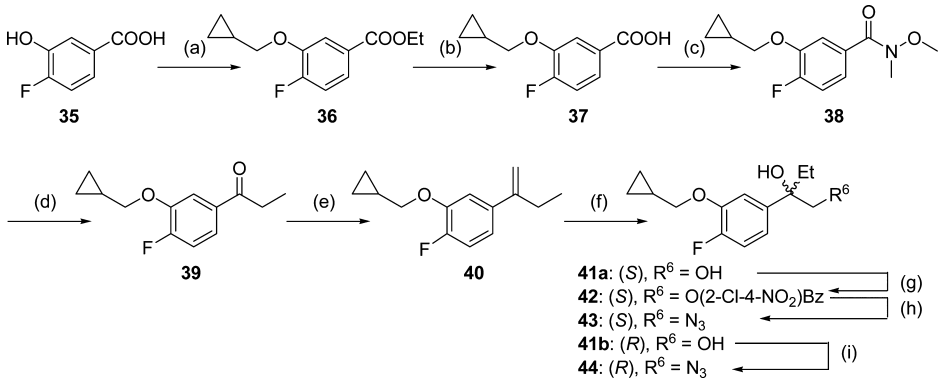

[a]Reagents and conditions: (a) H_2SO_4, EtOH, reflux, 4 h then (bromomethyl)cyclopropane, K_2CO_3, DMF, 90 °C, 5 h; (b) aq NaOH, EtOH, 60 °C, 4 h; (c) MeNHOMe·HCl, EDC·HCl, HOBt, TEA, DMF, room temp, 6 h; (d) EtMgBr, THF, room temp, 3 h; (e) $MePPh_3Br$, NaHMDS, THF, room temp, 12 h; (f) AD-mix*α* or AD-mix*β*, *t*-BuOH, H_2O, 0 °C, 3 h; (g) 2-Cl-4-NO_2-BzCl, TEA, CH_2Cl_2, room temp, 3 h; (h) aq NaOH, MeOH, 50 °C, 2 h then MsCl, TEA, CH_2Cl_2, room temp, 30 min then NaN_3, DMF, 90 °C, 12 h; (i) MsCl, TEA, CH_2Cl_2, room temp, 30 min then NaN_3, DMF, 90 °C, 12 h.

mix*β*, respectively. Intermediate **41a** was treated with 2-chloro-4-nitro-benzoylchloride to afford crystalline **42**, whose optical purity was improved to >99% ee by repeated crystallizations (three times). The benzoyl group of **42** was then removed by hydrolysis, and this was followed by sequential reactions with MsCl and NaN_3 to give azide **43**. Compound **41b** was directly converted to **44** without acylation and crystallization.

The 1,2,3-triazole derivatives were prepared by a ruthenium-catalyzed cycloaddition reaction[26] of alkyne intermediates (**9a**–**b**, **11**) with azide intermediates (**14a**–**e**, **22a**–**d**, **34a**–**i**, **43**, **44**) as shown in Scheme 6.

Scheme 6. General Synthetic Method for Preparation of Triazole Derivatives 45a–b (see Table 1), 46a–b (see Table 1), 47a–g (see Table 2), 48a–d (see Table 3), 49a–h (see Table 5) and 50a–d (see Table 6)[a]

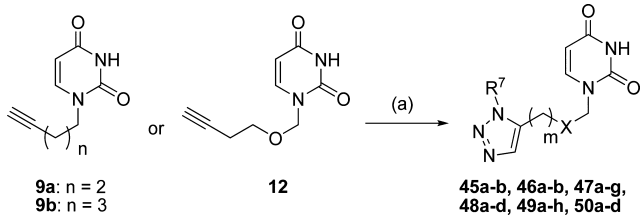

[a]Reagents and conditions: (a) azide, Cp*RuCl(COD), dioxane, 80 °C, 3 h. R7: various alkyl groups. X: CH_2 or O, m = 1 or 2

RESULTS AND DISCUSSION

Molecular Design and Synthesis of dUTPase Inhibitors Bearing a 1,2,3-Triazole Ring. The SAR studies of amide-containing uracil compounds revealed that *tert*-amide compound **6b** has almost 12-fold more improvement in the human dUTPase inhibitory activity over *sec*-amide compound **6a**. The ^{1}H NMR spectrum and NOE data of **6b** revealed that **6b** exists as a mixture of two conformational isomers at 25 °C (cis:trans = 2:3).[19] These results suggest that the cis conformation of **6b** should make an important contribution to its potency. To gain further evidence, we performed a docking study with human dUTPase and **6b** (cis isomer), and this suggested that the cis conformation of **6b** successfully interacts with the catalytic site of dUTPase based on the cocrystal structure of compound **7** and human dUTPase (PDB code 3ARA). (see Figure S1 in the Supporting Information). The modeling study showed that uracil and one of the terminal phenyl rings of **6b** were attributed to its potent and specific interaction with dUTPase. Accordingly, to improve the inhibitory potency, we designed a new scaffold with 1,5-disubstituted 1,2,3-triazoles as a viable amide surrogate for a locked cis conformation (Figure 2).[27,28] To carry out SAR studies focusing on the 1,2,3-triazole-containing uracil structure, we synthesized various uracil derivatives. We then examined in detail the influence of linker length and various *N*-alkyl moieties on the inhibitory activity.

Replacement of a *tert*-Amide Bond of 6b with a 1,2,3-Triazole Ring. First, we synthesized a 1,2,3-triazole derivative **45a** that corresponds to the *tert*-amide containing uracil derivative **6b** as a conformationally cis-locked compound (Figure 2). We also prepared analogues of **45a** to examine the effect of linker length on inhibitory potency (Table 1).

The human dUTPase inhibitory potency of the triazole-containing uracil derivative **45a** (IC_{50} = 1.3 μM) was comparable

Table 1. Human dUTPase Inhibitory Activity of Triazole-Containing Uracil Derivatives 45a–b, 46a–b, and *tert*-Amide Containing Uracil Compound 6b

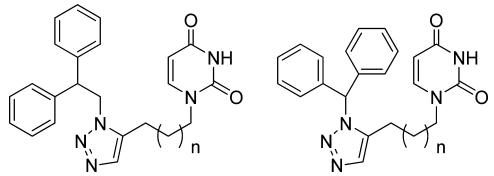

	IC_{50} (μM)[a]
6b	1.3 ± 0.068
45a	1.3 ± 0.052
45b	0.74 ± 0.011
46a	>10
46b	1.6 ± 0.019

[a]Enzyme inhibition assays are tested at 10 μM or below. IC_{50} values are shown as the mean ± SE (n = 3)

dx.doi.org/10.1021/jm3004174 | J. Med. Chem. 2012, 55, 6427–6437

to that of the *tert*-amide containing uracil compound **6b** (IC_{50} = 1.3 μM). Compound **45b** with a tetramethylene linker also showed potent inhibitory activity (IC_{50} = 0.74 μM). These data clearly showed that the inhibitory potency of **6b** is retained even if its *tert*-amide bond is replaced by the "cis-locked" 1,2,3-triazole ring and that both trimethylene and tetramethylene linkers are also applicable to triazole compounds. On the other hand, **46a–b**, having a 1-*N*-diphenylmethyl triazole moiety, had somewhat weaker inhibition potency compared to **45a–b** (IC_{50} = 1.6–10 μM).

Structural Simplification of the 2,2-Diphenylethyl Moiety of 45a–b and Substituent Effects of the Terminal Phenyl Ring. 1,2,3-Triazole-containing compounds such as **45a–b** showed potent enzyme inhibitory activity as expected. However, these compounds are not suitable as lead compounds owing to the following unfavorable properties: (1) relatively high molecular weight and (2) synthetic difficulties in various derivatization reactions due to the diphenyl ethyl moiety. Therefore, on the basis of the chemical structures of **45a–b** (Table 1), we next performed SAR study on the derivatives with a monophenylethyl moiety in order to solve these issues (Table 2).

Table 2. Human dUTPase Inhibitory Activity of Triazole-Containing Uracil Derivatives 47a–g and 45a–b

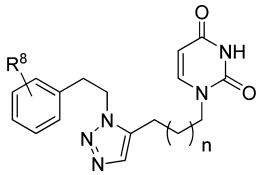

47a-g

	n	R^8	IC_{50} (μM)[a]
45a			1.3 ± 0.052
45b			0.74 ± 0.011
47a	1	H	>10
47b	2	H	3.5 ± 0.023
47c	2	2-MeO	5.7 ± 0.030
47d	2	3-MeO	4.1 ± 0.065
47e	2	4-MeO	>10
47f	2	2-(cyclopropyl)CH_2O	0.39 ± 0.0044
47g	2	3-(cyclopropyl)CH_2O	0.21 ± 0.0026

[a]Enzyme inhibition assays are tested at 10 μM or below. IC_{50} values are shown as the mean ± SE (n = 3)

The inhibitory potency of **47a** without one of the terminal phenyl group of **45a** is clearly diminished (IC_{50} > 10 μM). However, in the tetramethylene-linked series, the degree of reduced inhibitory potency of **47b** (almost 5-fold) was significantly smaller than that of **47a**. These data suggested that **47b** having the tetramethyene linker between the uracil ring and the triazole ring is a promising lead compound. Accordingly, we next synthesized compounds **47c–e**, which possess a methoxy group at various positions on the terminal phenyl ring of **47b**. The 2-methoxy derivative **47c** (IC_{50} = 5.7 μM) and 3-methoxy derivative **47d** (IC_{50} = 4.1 μM) retained moderate potency comparable to **47b**. On the other hand, the introduction of the methoxy group at the *p*-position of the terminal phenyl ring of **47b** diminished its inhibitory potency. We further designed and synthesized **47f–g** bearing a larger alkyloxy group such as a (cyclopropyl)methoxy group at the *o*- or *m*- position of its terminal phenyl ring. The resulting compounds both showed significantly potent inhibitory activity. In particular, **47g** (IC_{50} = 0.21 μM) showed almost 6-fold greater potency than the initial compound **45a**.

The Substituent Effect of Lower Alkyl Groups at the Benzylic Position of 47g on Inhibitory Potency. To improve the potency of **47g**, we investigated the effects of alkyl substitution at the benzylic position on inhibitory potency (Table 3). On the basis of the comparison of inhibitory potency

Table 3. Human dUTPase Inhibitory Activity of Triazole-Containing Uracil Derivatives 48a–d and 47g

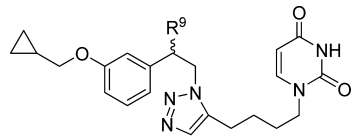

48a-d

	R^9	IC_{50} (μM)[a]
47g		0.21 ± 0.0026
48a	Me (*R*)	0.058 ± 0.0019
48b	Me (*S*)	0.87 ± 0.015
48c	Et (*R*)	0.029 ± 0.00047
48d	Et (*S*)	0.72 ± 0.022

[a]IC_{50} values are shown as the mean ± SE (n = 3)

of **45b** (IC_{50} = 0.74 μM) to **47b** (IC_{50} = 3.5 μM), we introduced some lower alkyl groups at the benzylic position of **47g** for further improvement in the inhibitory potency.

We synthesized compounds **48a–d**, by introduction of a methyl or ethyl group stereoselectively at the benzylic position of **47g**, and evaluated their potencies. From this evaluation, **48a** and **48c** having the *R* configuration were identified as highly potent inhibitors of human dUTPase (**48a**, IC_{50} = 0.057 μM; **48c**, IC_{50} = 0.029 μM). In contrast, **48b** and **48d** having the *S* configuration clearly exhibited weaker potency compared to the *R* isomers (**48b**, IC_{50} = 0.87 μM; **48d**, IC_{50} = 0.72 μM, eudismic ratio = 15–25).

A Solution to the Metabolic Instability of 48c and the Substituent Effects at the *m*- Position of the Terminal Phenyl Ring on Human dUTPase Inhibitory Activity. We next performed a pharmacokinetics study of the highly potent analogue **48c** to estimate its feasibility for in vivo evaluation via oral administration. From this study, we determined that **48c** was metabolically unstable in mice although its absorption was acceptable (Figure 4).

Although the metabolites of **48c** were not identified, we presumed that the instability of **48c** was associated with metabolism at its phenylethyl moiety. We expected that stereoselective introduction of a hydroxyl group into the benzylic position of **48c** should improve its metabolic stability in mice by preventing metabolism at the phenylethyl moiety. On the basis of this consideration, we synthesized **49a** and performed its pharmacokinetics study in mice. This study revealed that the metabolic stability of **49a** in mice was dramatically improved and the AUC value of **49a** was almost 15-fold higher than that of **48c** (Figure 5, Table 4). Fortunately, **49a** also retained its potent human dUTPase inhibitory activity (IC_{50} = 0.15 μM, Table 5) and its desirable lipophilicity (clogP 2.18).

We next designed and synthesized **49b–h** in order to optimize the enzyme inhibitory potency of the 1,2,3-triazole containing uracil derivatives and evaluated (Table 5). The results of this study showed that **49b** (IC_{50} = 0.21 μM), having a cyclopentyloxy group, and **49h** (IC_{50} = 0.15 μM), having a

dx.doi.org/10.1021/jm3004174 | *J. Med. Chem.* 2012, 55, 6427–6437

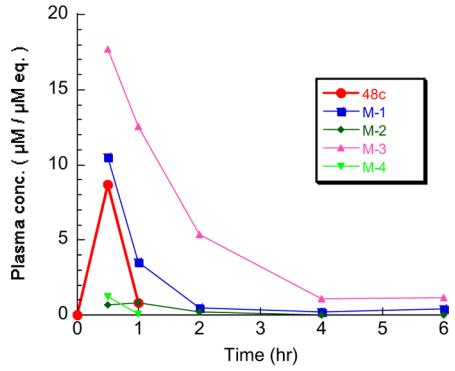

Figure 4. Pharmacokinetic profile of **48c** after oral administration dose at 50 mg/kg in Balb/cA mice (n = 2, ♂). Compound **48c** was administered as a solution (2.5% DMA, 2.5% Tween 80, 10% Cremophor EL). The pharmacokinetic parameters of **48c** are shown in Table 4. M-1, M-2, M-3, and M-4 represent the metabolites of **48c**. The HPLC analysis chart at 0.5 h after the oral administration is also shown in Figure S2 in the Supporting Information.

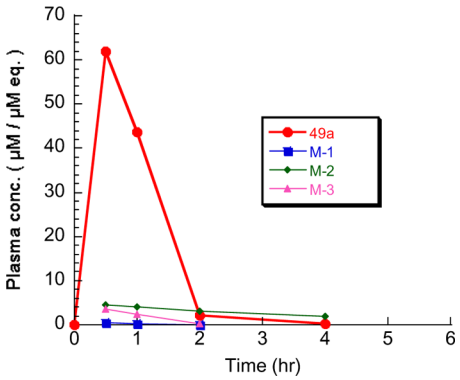

Figure 5. Pharmacokinetic profile of **49a** after oral administration dose at 50 mg/kg in Balb/cA mice (n = 2, ♂). Compound **49a** was administered as a solution (2.5% DMA, 2.5% Tween 80, 10% Cremophor EL). Pharmacokinetics parameters of **49a** are shown in Table 4. M-1, M-2, and M-3 represent the metabolites of **49a**. The HPLC analysis chart at 0.5 h after oral administration is also shown in Figure S2 in the Supporting Information.

Table 4. Pharmacokinetics Parameters of 48c and 49a after Oral Administration Dose at 50 mg/kg in Balb/cA mice (n = 2, ♂)[a]

	AUC_{0-t} (μM·h)	$T_{1/2}$ (h)	T_{max} (h)	C_{max} (μM)
48c	4.56	0.5−1	0.5	8.69
49a	67.37	1−2	0.5	62.06

[a]Each compound was administered as a solution (2.5% DMA, 2.5% Tween 80, 10% Cremophor EL).

(cyclobutyl)methoxy group, retained the inhibitory activity. However, none of these compounds had more potent inhibitory activity than **49a**.

Optimization of Compound 49a. To develop compounds with potent inhibitory activity and a desirable pharmacokinetic profile, we performed a SAR study of the derivatives of **49a**. Thus, we examined the influence of the linker between the uracil ring and the triazole ring, and the stereochemistry of benzylic position of **49a** (Table 6). Compound **50a** (distomer), which is an enantiomer of **49a** (eutomer), clearly exhibited weaker enzyme inhibitory potency (IC_{50} > 1.0 μM) as seen in the difference of potency of **48c** and **48d**. Compound **50b**, in which a methylene

Table 5. Human dUTPase Inhibitory Activity of Triazole-Containing Uracil Derivatives 49a−h

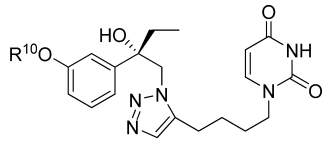

49a-h

	R^{10}	IC_{50} (μM)[a]
49a		0.15±0.0030
49b		0.21±0.0019
49c	Et	>1.0
49d		0.63±0.023
49e		0.55±0.026
49f		0.36±0.0083
49g		>1.0
49h		0.15±0.0027

[a]Enzyme inhibition assays are tested at 1.0 μM or below. IC_{50} values are shown as the mean ± SE (n = 3).

Table 6. Human dUTPase Inhibition Activity of Triazole-Containing Uracil Derivatives 50a−d and 49a[a]

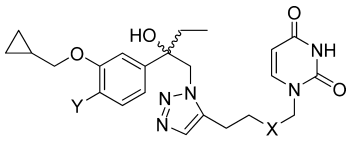

50a-d

	R or S	X	Y	IC_{50} (μM)[a]
49a	*S*	CH_2	H	0.15 ± 0.0030
50a	*R*	CH_2	H	>1.0
50b	*S*	O	H	0.17 ± 0.0074
50c	*S*	CH_2	F	0.067 ± 0.0017
50d	*R*	CH_2	F	0.35 ± 0.0049

[a]Enzyme inhibition assays are tested at 1.0 μM or below. IC_{50} values are shown as the mean ± SE (n = 3).

group of **49a** was replaced by an oxygen atom, showed potent inhibitory activity (IC_{50} = 0.17 μM) comparable to **49a**. We next examined compound **50c** having a fluoro group at the *p*-position of the terminal phenyl ring because the introduction of a fluoro group at the same position of sulfonamide-containing uracil compound **5** significantly increased its potency compared to the compound without the fluoro group in our previous report.[20] As we expected, compound **50c** showed highly potent inhibitory activity (IC_{50} = 0.067 μM, Table 6). The potency of *R* isomer **50d** (distomer) was weaker than that of *S* isomer **50c** (eutomer) (eudismic ratio = 5.2).

dx.doi.org/10.1021/jm3004174 | J. Med. Chem. 2012, 55, 6427−6437

Although the novel dUTPase inhibitors reported in this paper are not triphosphate mimics of a natural substrate dUTP, these compounds exhibited potent human dUTPase inhibitory activity. In particular, **48a**, **48c**, and **50c** exhibited high potency with IC_{50} values in the 10^{-8} M range. Such low IC_{50} value suggests that the active site of the enzyme can recognize these compounds better than the natural substrate dUTP (the concentration of a substrate dUTP in the enzyme inhibition assays is 0.1 μM). Therefore, elucidation of the enzyme inhibition mode by these compounds is crucial to discover further potent and clinical applicable inhibitors of human dUTPase. We previously described the cocrystal X-ray structure of pyrrolidylsulfonamide-containing uracil derivative **7** with human dUTPase.[19] This X-ray structure showed that the uracil ring of **7** occupies the uracil recognition region and that one of the terminal phenyl rings of **7** occupies a hydrophobic region which is formed by Val65, Ala90, Ala98, and Val112 residues of the active site and makes a stacking interaction with its own uracil ring (Figure S1 in the Supporting Information). From these results, the uracil rings and the terminal phenyl rings of these triazole-containing uracil derivatives were proposed to make similar interactions with human dUTPase. We further proposed that the high potency of eutomers (**48a**, **48c**, and **50c**) can be attributed to the efficient insertion of their phenyl ring into the hydrophobic region of the enzyme and that the improvement in potency observed by the introduction of a (cyclopropyl)methoxy group into the terminal phenyl ring can be attributed to an enhancement of hydrophobic interactions between the inhibitor and human dUTPase.

Human dUTPase Inhibitors Enhance the Growth Inhibition Activity of FdUrd in Vitro. We performed in vitro growth inhibition experiments with certain of our novel dUTPase inhibitors. These studies were done on HeLa S3 cells in combination with 5-fluoro-2′-deoxyuridine (FdUrd) to evaluate the chemotherapeutic enhancing effects of the dUTPase inhibitors. We performed cell proliferation assay by treatment with FdUrd at the concentration of 1 μM combined with various concentrations of the dUTPase inhibitors. T/C values (%) were obtained as the ratio of cell density determined by the crystal violet assay with drug treatment to without drug treatment for 24 h. To show the enhancement effect of the dUTPase inhibitor for growth inhibition activity of FdUrd, the EC_{50} (μM) value was calculated from concentration−T/C (%) curve as the concentration reducing the T/C (%) value by treatment with only FdUrd (T/C 70−80%) by half.

We selected four representative compounds (**45a**, **47g**, **48c**, **50c**) from each group of derivatives reported in this paper for evaluation of enhancement activity. These compounds exhibited feeble growth inhibition activity against HeLa S3 cell by themselves (EC_{50} = 23−100 μM). However, these compounds dramatically enhanced the growth inhibition activity of FdUrd (1 μM) against HeLa S3 cells (EC_{50} = 0.05−1.1 μM). Moreover, the degree of the enhancement correlated well with the potency of dUTPase inhibition. On the basis of these data, the ability of these compounds to enhance the growth inhibition mediated by FdUrd clearly can be ascribed to their ability to inhibit dUTPase in HeLa S3 cells.

Human dUTPase Inhibitor 50c Enhances the Antitumor Effect of 5-FU in Vivo. We performed a pharmacokinetics study on the highly potent dUTPase inhibitor **50c** to estimate the feasibility for an in vivo study of mice performed via oral administration. As expected, **50c** was well absorbed and metabolically stable in mice, comparable to the properties of **49a** (Figure 6, Table 8). Pharmacokinetics and enzyme inhibitory activity data (Table 6) showed that **50c** had a desirable profile for an in vivo study of mice and that the pharmacokinetic profile of **50c** (AUC: 57.3 μM·h) in mice was superior to that of **5** (AUC: 24.9 μM·h)[20] reported previously.

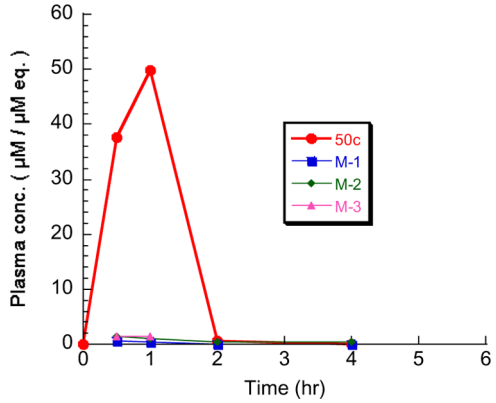

Figure 6. The pharmacokinetic profile of **50c** after oral administration dose at 50 mg/kg in Balb/cA mice (n = 2, ♂). Compound **50c** was administered as a solution (2.5% DMA, 2.5% Tween 80, 10% Cremophor EL). The pharmacokinetic parameters of **50c** are shown in Table 8. M-1, M-2, and M-3 represents the metabolites of **50c**.

We next evaluated the enhancing effect of **50c** for antitumor activity of 5-FU against in vivo breast cancer xenograft composed of MX-1 cells in vivo in mice. The details of the protocol for in vivo evaluation in mice are described in the Experimental Section. Compound **50c** alone exhibited no antitumor activity in vivo, which was consistent with feeble in vitro cytotoxicity of **50c** alone (Table 7). On the other hand, compound **50c** significantly enhanced the antitumor activity of 5-FU without significant body weight loss (Figure 7, Table 9).

Table 7. Enhancing Effect of dUTPase Inhibitors for Growth Inhibition Activity of FdUrd against HeLa S3 Cells in Vitro

	cytotoxicity EC_{50} (μM)[a]	EC_{50} (μM) With 1 μM FdUrd[b]	dUTPase IC_{50} (μM)[c]
45a	>100	1.1 ± 0.022	1.3 ± 0.052
47g	84 ± 2.1	0.26 ± 0.0046	0.21 ± 0.0026
48c	22 ± 0.13	0.05 ± 0.00049	0.029 ± 0.00047
50c	41 ± 0.25	0.07 ± 0.0013	0.067 ± 0.0017

[a]Cytotoxity of dUTPase inhibitors against HeLa S3 cells (72 h). [b]EC_{50} values show the concentration at which the dUTPase inhibitor reduces the T/C (%) value of FdUrd (1 μM, 70−80%) against HeLa S3 cells (24 h) by half. EC_{50} values are shown as the mean ± SE (n = 3). [c]IC_{50} values show dUTPase inhibitory activity as the mean ± SE (n = 3).

Table 8. Pharmacokinetics Parameters of 50c after Oral Administration Dose at 50 mg/kg in Balb/cA mice (n = 2, ♂)[a]

	AUC_{0-t} (μM·h)	$T_{1/2}$ (h)	T_{max} (h)	C_{max} (μM)
50c	57.28	1−2	1	49.80

[a]Compound **50c** was administered as a solution (2.5% DMA, 2.5% Tween 80, 10% Cremophor EL).

CONCLUSIONS

A 1,2,3-triazole-containing uracil compound **45a** was designed as an analogue of *tert*-amide-containing **6b** wherein the 1,2,3-

dx.doi.org/10.1021/jm3004174 | J. Med. Chem. 2012, 55, 6427−6437

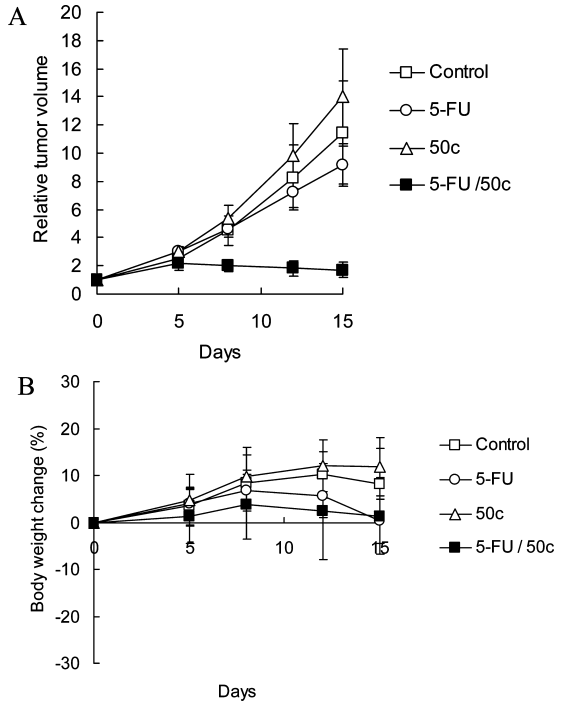

Figure 7. (A) Efficacy of **50c** for enhancing the antitumor activity of 5-FU against breast cancer xenograft MX-1 in mice. Relative tumor volume (RTV) is reported as mean ± SD of at least three independent experiments. (B) Body weight change (%) is expressed as mean ± SD.

triazole moiety mimics the amide bond of **6b** locked in a cis conformation. Compound **45a** possessed potent human dUTPase inhibitory activity, comparable to **6b**. We focused on **47b**, which is the monophenyl analogue of **45a**, as a lead compound because of its lower molecular weight and ease of the molecular modification. The SAR studies of the lead compound **47b** led to the discovery of **48a**, **48c**, and **50c**, which have high potency (IC_{50} = 0.029−0.067 μM). The affinity of these compounds for dUTPase was proposed to be superior to that of the natural substrate dUTP because their IC_{50} values were lower than the concentration of a substrate dUTP in the enzyme inhibition assays. These novel triazole-containing uracil derivatives markedly enhanced the growth inhibition activity of FdUrd against HeLa S3 cells in vitro with IC_{50} values in the 10^{-7}−10^{-8} M range. To the best of our knowledge, a pharmacokinetics study of **50c** in mice revealed that the AUC value of **50c** is the highest among the previously reported dUTPase inhibitors. It is noteworthy that **50c**, which exhibited high human dUTPase inhibitory potency and a desirable pharmacokinetic profile in mice, significantly enhanced the antitumor activity of 5-FU against the MX-1 xenograft model in mice. These data indicate that our novel dUTPase inhibitors should open the way to unprecedented beneficial chemotherapeutic strategies for cancer patients when used in combination with TS inhibitors.

EXPERIMENTAL SECTION

All commercially available starting materials and solvents were reagent grade. Silica gel column chromatography was performed on Merck silica gel 60 (230−400 mesh). ^{1}H NMR spectra were measured at 270 MHz on a JEOL JNM-EX270 or 400 MHz on a JEOL JNM-LA400. ^{13}C NMR spectra were measured at 100 MHz on a JEOL JNM-LA400. Chemical shifts were recorded in parts per million (ppm, δ) and were reported relative to the solvent peak or internal tetramethylsilane peak. High-resolution mass spectra (HRMS) were measured with a JEOL JMS-700 (FAB) or Waters micromass Q-Tof-2 (TOF). All NMR spectrum data and MS spectrum data of intermediates and tested compounds were presented in the Supporting Information. Chemical purities of the tested compounds were determined by combustion analysis or HPLC analysis and confirmed ≥95% purity. Combustion analyses (C, H, N) were performed on a Thermo Electron Corp. Flash EA 1112 series, and the values were within ±0.4% of the theoretical values and were presented in the Supporting Information. Chemical purities of some tested compounds were determined by HPLC analysis with a SHIMADZU Prominence HPLC system, and the values are presented in the Supporting Information. Optical rotations were measured by a HORIBA SEPA-200 polarimeter and are presented in the Supporting Information. The clogP values were calculated using the ACD/LogP algorithm (ACD/Laboratories release 10.00, version 10.01).

dUTPase Inhibition Assay. In vitro dUTPase inhibition assays were conducted by measuring the production of [5-^{3}H]dUMP from [5-^{3}H]dUTP according to the reported method.[19] Briefly, a total of 0.2 mL solution, containing 0.02 mL of 1 μM dUTP (including 588 Bq/mL [5-^{3}H]dUTP), 0.05 mL of a 0.2 M Tris buffer solution (pH 7.4), 0.05 mL of 16 mM magnesium chloride, 0.02 mL of 20 mM 2-mercaptoethanol, 0.02 mL of a 1% aqueous solution of fetal bovine serum-derived albumin, 0.02 mL of varying concentrations of test compound solutions or pure water as a control, and 0.02 mL of a solution of human dUTPase, was reacted at 37 °C for 15 min. After the reaction, the solution was immediately heated at 100 °C for 1 min to terminate the reaction, followed by centrifugation at 15000 rpm for 2 min. An aliquot (150 μL) of the supernatant thus obtained by centrifugation was analyzed using an Atlantis dC18 column (manufactured by Waters Corp., 4.6 mm × 250 mm) and high-performance liquid chromatography (manufactured by Shimadzu Corp., Prominence). The inhibitory rate of the compound was calculated from the formula shown below. IC_{50} (μM), which the concentration of the inhibitor yielding 50% inhibition rate, was obtained from the concentration−inhibitory rate curve.

Table 9. in Vivo Enhancing Efficacy of 50c for Antitumor Activity of 5-FU against Breast Cancer Xenograft MX-1 in Mice

	dose (mg/kg/day)	treatment	TV[a] (mm^3, mean ± SD)	RTV[b] (mean ± SD)	IR[c] (%)
control			2047.62 ± 693.70	11.41 ± 3.74	
5-FU	15	ci	1644.48 ± 322.60	9.13 ± 1.35	20.0
50c	300	po	2474.95 ± 534.68	14.06 ± 3.35	−23.2
5-FU/**50c**	15/300	ci/po	300.68 ± 103.20	1.72 ± 0.55[d]	84.9

[a]Tumor volume (TV) on day 15 was calculated according to the following formula: TV (mm^3) = [(width)^2 × (length)]/2. [b]Relative tumor volume (RTV) on day 15 was calculated as the ratio of TV on day 15 to that on day 0 according to the following formula: RTV = (TV on day 15)/(TV on day 0). [c]Inhibition rate (IR) of tumor growth on day 15 based on the RTV was calculated according to the following formula: IR (%) = [1 − (mean RTV of the treated group)/(mean RTV of the control group)] × 100. [d]**: $p < 0.01$ Dunnet test as compared with the control group. ##: $p < 0.01$ Student's t test as compared with the 5-FU group.

dx.doi.org/10.1021/jm3004174 | J. Med. Chem. 2012, 55, 6427−6437

$$\text{inhibitory rate (\%)} = [1 - (\text{amount of } [5\text{-}^3\text{H}]\text{dUMP in presence of test solution (dpm)}) / (\text{amount of } [5\text{-}^3\text{H}]\text{dUMP as control (dpm)})] \times 100$$

Evaluation of in Vitro Cytotoxicity. HeLa S3 cells (human ovarian carcinoma) were grown in the RPMI1640 medium supplemented with 10% fetal bovine serum (FBS). Exponentially growing cells were seeded in 96-well plates (1500 cells/0.18 mL) and incubated at 37 °C in a humidified 5% CO_2 atmosphere. After 24 h, various concentration of test compounds were added to the corresponding plates at the volume of 20 μL per well, the plates were incubated for 72 h, and then cell proliferation was determined by the crystal violet assay. Optical density at 540 nm (OD_{540}) was measured by a plate reader. Then, we calculated the T/C (%) value which is the ratio of the OD_{540} with drug treatment to without drug [T/C (%) = (OD_{540} of treated well/OD_{540} of nontreated well) × 100]. The EC_{50} (μM) for the cytotoxicity of the test compound was the concentration yielding 50% T/C value, which was calculated from the concentration−T/C (%) curve.

Evaluation of the Enhancement of the Growth Inhibition Activity of FdUrd in Vitro. HeLa S3 cells were seeded in 96-well plates (1500 cells/0.18 mL) and incubated at 37 °C in a humidified 5% CO_2 atmosphere as described above. After 24 h, five different concentrations of test compounds and FdUrd (1 μM) were added to the corresponding plates at the volume of 20 μL per well. After 24 h incubation, thymidine (30 μM) was added to the plates at the volume of 10 μL per well. After further 48 h incubation, the cell density was measured and the T/C (%) values were obtained as mentioned above. The EC_{50} for the enhancement of the growth inhibition activity of FdUrd was calculated from the concentration−T/C (%) curve as the concentration at which the test compound reduced the T/C (%) value for the treatment of 1 μM FdUrd by half.

Ethics Statement. All animal experiments were performed with the approval of the Animal Ethics Committees of Animal Care and Use.

Evaluation of Pharmacokinetics Profile. Balb/cA mice were also used to study the pharmacokinetic properties of the inhibitors. Male Balb/cA mice were supplied by CLEA Japan, Inc. (Tokyo, Japan). Blood samples were collected at five time points (30 min, 1 h, 2 h, 4 h, 6 h) after a single oral dose of 50 mg/kg inhibitor in a solution (2.5%DMA, 2.5% Tween 80, 10% Cremophor EL). The quantitation of inhibitor plasma levels was analyzed by reverse-phase ultraperformance liquid chromatography (0.35 mL/min 10 mM ammonium acetate/acetonitrile gradient, 10 cm, 2.1 mm i.d. Acquity BEH Shield RP18 column, UV detection 268 or 270 nm). Ultraperformance liquid chromatography condition was shown in below.

System: Waters ultraperformance liquid chromatography
Column: ACQUITY BEH Shield RP18 2.1 mm × 100 mm
Column temperature: 40 °C
Mobile phase: A = 10 mM ammonium acetate, B = acetonitrile
Flow rate: 0.35 mL/min
Detection: UV 268 or 270 nm
Gradient condition:

min	A (%)	B (%)
0.00	95	5
0.40	95	5
6.00	20	80
6.50	20	80
6.51	95	5
9.00	95	5

The pharmacokinetic parameters were derived from the mean plasma concentrations at each time point using the WinNonlin computer program (Pharsight).

Evaluation of Antitumor Efficacy of Compound 50c. Balb/cA JcL-nu mice (five weeks of ages) were obtained from Clea Japan, Inc. (Tokyo, Japan). MX-1 human breast carcinoma (Japanese Foundation For Cancer Research) was maintained by subcutaneous (sc) transplantation in mice. For the experiment, tumors were excised and fragments (~2 mm in diameter) were implanted subcutaneously by trocar with fragment of human tumor. After implantation, the animals were divided into four groups and treated with either vehicle (2.5% DMA, 2.5% Tween 80, 10% cremophor EL, and 0.5% HPMC), 5-FU (15 mg/kg/day) by continuous infusion using osmotic pump for 14 days, compound **50c** (300 mg/kg/day, once daily) by po for 14 days, or a combination of 5-FU (15 mg/kg/day) and compound **50c** (300 mg/kg/day, once daily) for 14 days. Tumor size and body weight were measured twice a week. Tumor volume (TV) were estimated with the formula: TV (mm^3) = length (mm) × width (mm) × width (mm) × 0.5. Relative tumor volume (RTV) on day 15 was calculated as the ratio of TV on day 15 to that on day 0 according to the following formula: RTV = (TV on Day 15)/(TV on Day 0). The inhibition rate of tumor growth on day 15 on the basis of RTV was calculated according to the following formula:

$$\text{inhibition rate (\%)} = \left(1 - \frac{\text{mean RTV of the treated group}}{\text{mean RTV of the control group}}\right) \times 100$$

The body weight change was calculated according to the following formula:

$$\text{body weight change (\%)} = \frac{[(\text{body weight}) - (\text{body weight on day 0})]}{(\text{body weight on day 0})} \times 100$$

■ ASSOCIATED CONTENT

Ⓢ Supporting Information

Experimental details and analytical data for intermediates and test compounds, details of the binding model of **6b** with human dUTPase, and HPLC charts of the pharmacokinetics studies described in the article. This material is available free of charge via the Internet at http://pubs.acs.org.

■ AUTHOR INFORMATION

Corresponding Author

*Phone: 81-29-865-4527. Fax: 81-29-865-2170. E-mail: m-fukuoka@taiho.co.jp.

Notes

The authors declare no competing financial interest.

■ ACKNOWLEDGMENTS

We thank Dr. K. L. Kirk (NIDDK, NIH), Dr. Tadafumi Terada (Taiho Pharmaceutical Co. Ltd.), and Dr. Kazuharu Noguchi (Taiho Pharmaceutical Co. Ltd.) for very helpful suggestions and Satoko Tanaka, Emi Inaba, and the staff of the Drug Discovery Research Center of Taiho Pharmaceutical Co. Ltd. for their technical assistance.

■ ABBREVIATIONS USED

dUTPase, deoxyuridine triphosphatase; TS, thymidylate synthase; 5-FU, 5-fluorouracil; dUTP, deoxyuridine triphosphate; dUMP, deoxyuridine monophosphate; dTMP, thymidine monophosphate; dTTP, thymidine triphosphate; FdUTP, 5-fluoro-2′-deoxyuridine triphosphate; $(TMS)_2$Ura, bistrimethylsilyluracil; DIAD, diisopropyl azodicarboxylate; DIEA, *N*-ethyldiisopropylamine; NaHMDS, sodium bis(trimethylsilyl)amide; EDC·HCl, *N*-(3-dimethylaminopropyl)-*N*′-ethylcarbodiimide hydrochloride; HOBt, 1-hydroxybenzotriazole; TEA, triethylamine; Cp*RuCl(COD), chloro(pentamethylcyclopentadienyl)-(cyclooctadiene)ruthenium(II); FdUrd, 5-fluoro-2′-deoxyuridine; SE, standard error; SD, standard deviation; TV, tumor

volume; RTV, relative tumor volume; IR, inhibition rate; FBS, fetal bovine serum; HPMC, hydroxypropyl methylcellulose

REFERENCES

(1) Mol, C. D.; Harris, J. M.; McIntosh, E. M.; Tainer, J. A. Human dUTP pyrophosphatase: uracil recognition by a beta hairpin and active sites formed by three separate subunits. *Structure* **1996**, *4*, 1077−1092.

(2) McIntosh, E. M.; Haynes, R. H. dUTP pyrophosphatase as a potential target for chemotherapeutic drug development. *Acta Biochim. Pol.* **1997**, *44*, 159−171.

(3) Longley, D. B.; Harkin, D. P.; Johnston, P. G. 5-Fluorouracil: mechanisms of action and clinical strategies. *Nature Rev. Cancer* **2003**, *3*, 330−338.

(4) Curtin, N. J.; Harris, A. L.; Aherne, G. W. Mechanism of cell death following thymidylate synthase inhibition: 2′-deoxyuridine-5′-triphosphate accumulation, DNA damage, and growth inhibition following exposure to CB3717 and dipyridamole. *Cancer Res.* **1991**, *51*, 2346−2352.

(5) Webley, S. D.; Hardcastle, A.; Ladner, R. D.; Jackman, A. L.; Aherne, G. W. Deoxyuridine triphosphatase (dUTPase) expression and sensitivity to the thymidylate synthase (TS) inhibitor ZD9331. *Br. J. Cancer* **2000**, *83*, 792−799.

(6) An, Q.; Robins, P.; Lindahl, T.; Barnes, D. E. 5-Fluorouracil incorporated into DNA is excised by the Smug1 DNA glycosylase to reduce drug cytotoxicity. *Cancer Res.* **2007**, *67*, 940−945.

(7) Wilson, P. M.; Fazzone, W.; LaBonte, M. J.; Deng, J.; Neamati, N.; Ladner, R. D. Novel opportunities for thymidylate metabolism as a therapeutic target. *Mol. Cancer Ther.* **2008**, *7*, 3029−3037.

(8) Ingraham, H. A.; Tseng, B. Y.; Goulian, M. Nucleotide levels and incorporation of 5-fluorouracil and uracil into DNA of cells treated with 5-fluorodeoxyuridine. *Mol. Pharmacol.* **1982**, *21*, 211−216.

(9) Zalud, P.; Wachs, W. O.; Nyman, P. O.; Zeppezauer, M. M. Inhibition of the proliferation of human cancer cells in vitro by substrate-analogous inhibitors of dUTPase. *Adv. Exp. Med. Biol.* **1994**, *370*, 135−138.

(10) Persson, T.; Larsson, G.; Nyman, P. O. Synthesis of 2′-deoxyuridine 5′-(alpha,beta-imido) triphosphate: a substrate analogue and potent inhibitor of dUTPase. *Bioorg. Med. Chem.* **1996**, *4*, 553−556.

(11) Nguyen, C.; Kasinathan, G.; Leal-Cortijo, I.; Musso-Buendia, A.; Kaiser, M.; Brun, R.; Ruiz-Perez, L. M.; Johansson, N. G.; Gonzalez-Pacanowska, D.; Gilbert, I. H. Deoxyuridine triphosphate nucleotidohydrolase as a potential antiparasitic drug target. *J. Med. Chem.* **2005**, *48*, 5942−5954.

(12) Whittingham, J. L.; Leal, I.; Nguyen, C.; Kasinathan, G.; Bell, E.; Jones, A. F.; Berry, C.; Benito, A.; Turkenburg, J. P.; Dodson, E. J.; Ruiz Perez, L. M.; Wilkinson, A. J.; Johansson, N. G.; Brun, R.; Gilbert, I. H.; Gonzalez Pacanowska, D.; Wilson, K. S. dUTPase as a platform for antimalarial drug design: structural basis for the selectivity of a class of nucleoside inhibitors. *Structure* **2005**, *13*, 329−338.

(13) Nguyen, C.; Ruda, G. F.; Schipani, A.; Kasinathan, G.; Leal, I.; Musso-Buendia, A.; Kaiser, M.; Brun, R.; Ruiz-Perez, L. M.; Sahlberg, B. L.; Johansson, N. G.; Gonzalez-Pacanowska, D.; Gilbert, I. H. Acyclic nucleoside analogues as inhibitors of *Plasmodium falciparum* dUTPase. *J. Med. Chem.* **2006**, *49*, 4183−4195.

(14) Jiang, Y. L.; Chung, S.; Krosky, D. J.; Stivers, J. T. Synthesis and high-throughput evaluation of triskelion uracil libraries for inhibition of human dUTPase and UNG2. *Bioorg. Med. Chem.* **2006**, *14*, 5666−5672.

(15) Mc Carthy, O. K.; Schipani, A.; Buendia, A. M.; Ruiz-Perez, L. M.; Kaiser, M.; Brun, R.; Pacanowska, D. G.; Gilbert, I. H. Design, synthesis and evaluation of novel uracil amino acid conjugates for the inhibition of *Trypanosoma cruzi* dUTPase. *Bioorg. Med. Chem. Lett.* **2006**, *16*, 3809−3812.

(16) Beck, W. R.; Wright, G. E.; Nusbaum, N. J.; Chang, J. D.; Isselbacher, E. M. Enhancement of methotrexate cytotoxicity by uracil analogues that inhibit deoxyuridine triphosphate nucleotidohydrolase (dUTPase) activity. *Adv. Exp. Med. Biol.* **1986**, *195* (Pt B), 97−104.

(17) Marriott, J. H.; Aherne, G. W.; Hardcastle, A.; Jarman, M. Synthesis of certain 2′-deoxyuridine derivatives containing substituted phenoxy groups attached to C-5′; evaluation as potential dUTP analogues. *Nucleosides, Nucleotides Nucleic Acids* **2001**, *20*, 1691−1704.

(18) Hampton, S. E.; Baragana, B.; Schipani, A.; Bosch-Navarrete, C.; Musso-Buendia, J. A.; Recio, E.; Kaiser, M.; Whittingham, J. L.; Roberts, S. M.; Shevtsov, M.; Brannigan, J. A.; Kahnberg, P.; Brun, R.; Wilson, K. S.; Gonzalez-Pacanowska, D.; Johansson, N. G.; Gilbert, I. H. Design, synthesis, and evaluation of 5′-diphenyl nucleoside analogues as inhibitors of the *Plasmodium falciparum* dUTPase. *ChemMedChem* **2011**, *6*, 1816−1831.

(19) Miyakoshi, H.; Miyahara, S.; Yokogawa, T.; Chong, K. T.; Taguchi, J.; Endoh, K.; Yano, W.; Wakasa, T.; Ueno, H.; Takao, Y.; Nomura, N.; Shuto, S.; Nagasawa, H.; Fukuoka, M. Synthesis and discovery of *N*-carbonylpyrrolidine- or *N*-sulfonylpyrrolidine-containing uracil derivatives as potent human deoxyuridine triphosphatase. *J. Med. Chem.* **2012**, *55*, 2960−2969.

(20) Miyahara, S.; Miyakoshi, H.; Yokogawa, T.; Taguchi, J.; T., M.; Endoh, K.; Yano, W.; Wakasa, T.; Ueno, H.; Takao, Y.; Fujioka, A.; Hashimoto, A.; Itou, K.; Yamamura, K.; Nomura, M.; Nagasawa, H.; Shuto, S.; Fukuoka, M. Discovery of a novel class of potent human deoxyuridine triphosphatase inhibitors remarkably enhancing the antitumor activity of thymidylate synthase inhibitors. *J. Med. Chem.* **2012**, *55*, 2970−2980.

(21) Miyahara, S.; Miyakoshi, H.; Yokogawa, T.; Chong, K. T.; Taguchi, J.; Muto, T.; Endoh, K.; Yano, W.; Wakasa, T.; Ueno, H.; Takao, Y.; Fujioka, A.; Hashimoto, A.; Itou, K.; Yamamura, K.; Nomura, M.; Nagasawa, H.; Shuto, S.; Fukuoka, M. Discovery of highly potent human deoxyuridine triphosphatase inhibitors based on the conformation restriction strategy. *J. Med. Chem.* **2012**, *55*, 5483−5496.

(22) Ahn, H.; Choi, T. H.; De Castro, K.; Lee, K. C.; Kim, B.; Moon, B. S.; Hong, S. H.; Lee, J. C.; Chun, K. S.; Cheon, G. J.; Lim, S. M.; An, G. I.; Rhee, H. Synthesis and evaluation of *cis*-1-[4-(hydroxymethyl)-2-cyclopenten-1-yl]-5-[(124)I]iodouracil: a new potential PET imaging agent for HSV1-tk expression. *J. Med. Chem.* **2007**, *50*, 6032−6038.

(23) Kumar, S.; Hundal, G.; Paul, D.; Hundal, M. S.; Singh, H. Heterocalixarenes. 1. Calix[2]uracil[2]arene: Synthesis, X-ray structure, Conformational Analysis, and Binding Character. *J. Org. Chem.* **1999**, *64*, 7717−7726.

(24) Mori, K. Synthesis of (*R*)-ar-Turmerone and its conversion to (*R*)-ar-himachalene, a pheromone component of the flea beetle: (*R*)-ar-himachalene is dextrorotary in hexane, while levorotatory in chloroform. *Tetrahedron: Asymmetry* **2005**, *16*, 685−692.

(25) Spino, C.; Beaulieu, C.; Lafreniere, J. Chiral alpha-substituted carbonyls and alcohols from the S(N)2′ displacement of cuprates on chiral carbonates: an alternative to the alkylation of chiral enolates. *J. Org. Chem.* **2000**, *65*, 7091−7097.

(26) Zhang, L.; Chen, X.; Xue, P.; Sun, H. H.; Williams, I. D.; Sharpless, K. B.; Fokin, V. V.; Jia, G. Ruthenium-catalyzed cycloaddition of alkynes and organic azides. *J. Am. Chem. Soc.* **2005**, *127*, 15998−15999.

(27) Tam, A.; Arnold, U.; Soellner, M. B.; Raines, R. T. Protein Prosthesis: 1,5-Disubstituted[1,2,3]triazoles as *cis*-Peptide Bond Surrogates. *J. Am. Chem. Soc.* **2007**, *129*, 12670−12671.

(28) Horne, W. S.; Olsen, C. A.; Beierle, J. M.; Montero, A.; Ghadiri, M. R. Probing the Bioactive Conformation of an Archetypal Natural Product HDAC Inhibitor with Conformationally Homogeneous Triazole-Modified Cyclic Tetrapeptides. *Angew. Chem., Int. Ed.* **2009**, *48*, 4718−4724.